Bulletin of the New Zealand Society for Earthquake Engineering, Vol. 48, No. 2, June 2015

SUPPLEMENTAL DAMPERS IN BASE-ISOLATED BUILDINGS TO MITIGATE LARGE ISOLATOR DISPLACEMENT UNDER EARTHQUAKE EXCITATIONS

Daniel H. Zelleke[1*], Said Elias[2], Vasant A. Matsagar[3] and Arvind K. Jain[4]

(Submitted *September 2014*; Reviewed *October 2014*; Accepted *November 2014*)

ABSTRACT

The effect of viscous, viscoelastic, and friction supplemental dampers on the seismic response of base-isolated building supported by various isolation systems is investigated. Although base-isolated buildings have an advantage in reducing damage to the superstructure, the displacement at the isolation level is large, especially under near-fault ground motions. The influence of supplemental dampers in controlling the isolator displacement and other responses of base-isolated building is investigated using a multi-storey building frame. The coupled equations of motion are derived, solved and time history analysis is carried out on a building modeled with fifteen combinations of five isolation systems and three passive dampers. The seismic responses are compared with that of the fixed-base and base-isolated buildings. Based on the results, it is concluded that supplemental dampers are beneficial to control the large deformation at the isolator level. Parametric study is conducted and optimum ranges of damper parameters to achieve reduced isolator displacement without adverse effect on the other responses are determined. Further, it is concluded that the combination of the resilient-friction base isolator (R-FBI) and viscous damper is the most effective in reducing the bearing displacement without significant increase in superstructure forces.

INTRODUCTION

Base isolation is an earthquake resistant design technique in which the superstructure is isolated from ground movement to reduce the transfer of seismic forces. The superstructure is isolated from the foundation by isolation bearings having very low lateral stiffness which shifts the fundamental time period of the building to a higher value. This shift in the time period results in fundamental frequency of the building much lower than the predominant frequencies of the ground motion, thereby significantly reducing the earthquake energy transmitted to the building [1-2].

Base isolation protects both structural as well as non-structural components from suffering damage due to earthquake and helps structures to remain in service even after a large earthquake event. This makes the technique preferred for earthquake resistant design, especially for areas with large seismic loading. Various isolation techniques were proposed on which a number of analytical and experimental investigations were conducted demonstrating the suitability of the isolation techniques for earthquake resistant design of structures [3-10]. Base isolation, currently, is one of the popular earthquake resistant design techniques for important structures like hospitals, schools, industrial structures, nuclear power plants etc.

Different researchers [11-13] showed that the isolator displacement in base-isolated buildings is very large under near-fault ground motions due to the long pulse characteristics of this type of earthquakes and the base-isolated buildings are flexible due to incorporation of bearings with low horizontal stiffness. The increased isolator displacement is a concern in seismic isolation and needs to be addressed. Increased isolator displacement mandates providing larger moat widths and design of flexible services to the base-isolated building. Both these requirements lead to increased costs, which can be reduced by controlling the excessively large isolator displacements. Jangid and Kelly [12] showed that the bearing displacement under near-fault motion decreases with the increase in the isolation damping. Optimum lead-rubber bearings and friction pendulum systems under near-fault ground motions were also determined by Jangid [14-15].

Various other techniques were suggested to lessen the excessively large isolator displacement in base-isolated structures by different researchers [16-19]. Chang et al. [20], Kim et al. [21], Lu and Lin [22], Providakis [23], Lu et al. [24], Oh et al. [25] and Qin et al. [26] also conducted experimental and analytical studies and indicated that supplemental damping can be effective in mitigating the undesirable effects of near-fault ground excitations. Further studies which detail the effectiveness and optimum parameters of the supplemental dampers used in connection with mitigation of large isolator displacement in base-isolated buildings with various isolation systems under near-fault and far-fault ground motions are beneficial. Therefore, it would be useful to investigate the effects of applying supplemental viscous, viscoelastic, and friction dampers in reducing the isolator displacement in base-isolated buildings subjected to near-fault and far-fault ground motions.

This paper investigates the influence and effectiveness of using supplemental viscous, viscoelastic, and friction dampers on the response of base-isolated buildings under near-fault and far-fault ground motions. The main objectives of the study are: (i) to study the effect of supplemental viscous, viscoelastic, and friction dampers on the seismic response of base-isolated buildings with various elastomeric and sliding isolation systems, (ii) to conduct parametric study to obtain optimum ranges of parameters for which each of the dampers are most

[1] *Corresponding Author, Postgraduate Student, Dept. of Civil Engg., Indian Institute of Technology (IIT) Delhi, New Delhi, danihabt@gmail.com.*
[2] *Research Scholar, Dept. of Civil Engg., Indian Institute of Technology (IIT) Delhi, New Delhi, said.elias@civil.iitd.ac.in.*
[3] *Associate Professor, Dept. of Civil Engg., Indian Institute of Technology (IIT) Delhi, New Delhi, matsagar@civil.iitd.ac.in.*
[4] *Professor, Dept. of Civil Engg., Indian Institute of Technology (IIT) Delhi, New Delhi, akjain@civil.iitd.ac.in.*

effective, and (iii) to compare the effectiveness of each of the combinations of the isolation systems and supplemental damping devices with respect to controlling the isolator displacement without adversely affecting other responses of the base-isolated building.

MODELING OF BASE-ISOLATED BUILDING WITH DAMPER

The idealized mathematical models of the multi-storey building considered for the present study are shown in Figure 1. Figures 1(a) and 1(b), respectively, show the models for fixed-base and base-isolated buildings while Figure 1(c) depicts the model for base-isolated building with supplemental damper connected at the base mass level. Schematic representations for five isolation systems, such as laminated rubber bearing (LRB), lead-rubber bearing i.e. New Zealand (N-Z) system, pure friction system (PF), friction pendulum system (FPS) and resilient-friction base isolator (R-FBI), are shown in Figures 2(a) to 2(e), respectively, while the force-deformation relations for the three supplemental dampers used in the present study, such as viscous damper (VD), viscoelastic damper (VED), and friction damper (FD), are shown in Figures 2(f) to 2(h), respectively. The schematic representations of isolation systems give an idea about their behavior and mathematical modeling, whereas, the force-deformation relations for dampers give an idea about their energy dissipating characteristics. The following assumptions are made in modeling the building:

1. The building is modeled as a shear frame considering only one lateral degree of freedom at each floor level.
2. The mass of the structure is lumped at each floor level and the floors are considered to be infinitely stiff in their own plane.
3. The columns providing the lateral stiffness are assumed to be axially inextensible.
4. The effects of soil-structure interaction are neglected.
5. Only one horizontal component of the earthquake ground motion is applied to the building at a time.
6. Taking into account the fact that base isolation reduces the earthquake response of structures helping the elastic limit not to be exceeded in the superstructure, the analysis is carried out under the reasonable assumption that the building frame remains within the elastic range under the excitations from the ground motions.

A uniform damping ratio (ξ_s) of 0.02 is taken for the superstructure. All floor masses are taken to be equal and the floor stiffness are decided in such a way that a required fundamental time period of the fixed-base building (T) is obtained. For this study, all stories are considered to have the same lateral stiffness, and base mass (m_b) of the base-isolated building model is taken to be equal to the floor masses.

Different combinations of the five isolators and three supplemental dampers are investigated herein. The dampers are connected at the isolation level with one end connected to the base mass and the other to the ground. The fixed-base and base-isolated building models are also studied for comparison purpose.

Laminated Rubber Bearing (LRB)

Steel and rubber plates built in the alternate layers are the basic components of laminated rubber bearings [2]. The restoring force (F_b) developed in the laminated rubber bearing is given by

$$F_b = c_b \dot{x}_b + k_b x_b \tag{1}$$

where c_b and k_b are the damping coefficient and the stiffness of the isolation system which are selected to provide specific values of damping ratio (ξ_b) and isolation period (T_b), respectively, using the following expressions

$$c_b = 2\xi_b m \omega_b \tag{2}$$

$$k_b = m\left(\frac{2\pi}{T_b}\right)^2 \tag{3}$$

where $m = m_b + \sum_{j=1}^{N} m_j$ is the total mass of the base-isolated building, m_j is the mass of j^{th} floor, and $\omega_b = 2\pi / T_b$ is the isolation frequency.

Lead-Rubber Bearing (New Zealand, N-Z System)

Lead-rubber bearings are similar to the LRB with additional central lead-core provided as a means of additional energy dissipation [2]. It also provides initial rigidity against wind loads and minor earthquakes. The force-deformation behavior of the lead-rubber bearing is non-linear hysteretic. The restoring force (F_b) developed in the isolation system is given by

$$F_b = c_b \dot{x}_b + \alpha k_i x_b + (1-\alpha) F_y Z \tag{4}$$

where F_y is the yield strength of the bearing, α is the ratio of post-yield to pre-yield stiffness of the bearing, k_i is the initial stiffness of the bearing, and Z is a non-dimensional hysteretic displacement component satisfying a non-linear differential equation of first order expressed as $q\dot{Z} = A\dot{x}_b + \beta|\dot{x}_b||Z|Z|^{n-1} - \tau\dot{x}_b|Z|^n$ [27]. In this equation, q is the yield displacement while β, τ, and A are dimensionless parameters selected to be 0.5, 0.5 and 1, respectively. The parameter n controls the smoothness of transition from elastic to plastic range and is taken as 2.

The isolation period (T_b), damping ratio (ξ_b), and normalized yield strength ($F_o = F_y/W$) are the parameters used to characterize the lead-rubber bearing (where $W = mg$ is the total weight of the base-isolated building and g is the acceleration due to gravity). The damping coefficient (c_b) and the isolation stiffness (k_b) of the N-Z system are defined using Equations 2 and 3, respectively.

Pure Friction System (PF)

In PF system, the horizontal friction force provides resistance to lateral motion and dissipates energy. The PF system is represented here using Coulomb's friction with friction coefficient (μ). The limiting friction force in the isolation system is $F_L = \mu W$. The isolation system will be in stick or slip mode depending on the frictional force $(F_x = x_b k_i)$ with negligibly small yield displacement (q). The restoring force (F_b) in the stick phase (i.e. $F_x < F_L$) is given by

$$F_b = F_x . \tag{5}$$

The frictional force increases up to a maximum value of F_L at which point the isolation system will be in slip mode. The restoring force in the slip phase is given by

$$F_b = F_L \operatorname{sgn}(\dot{x}_b) . \tag{6}$$

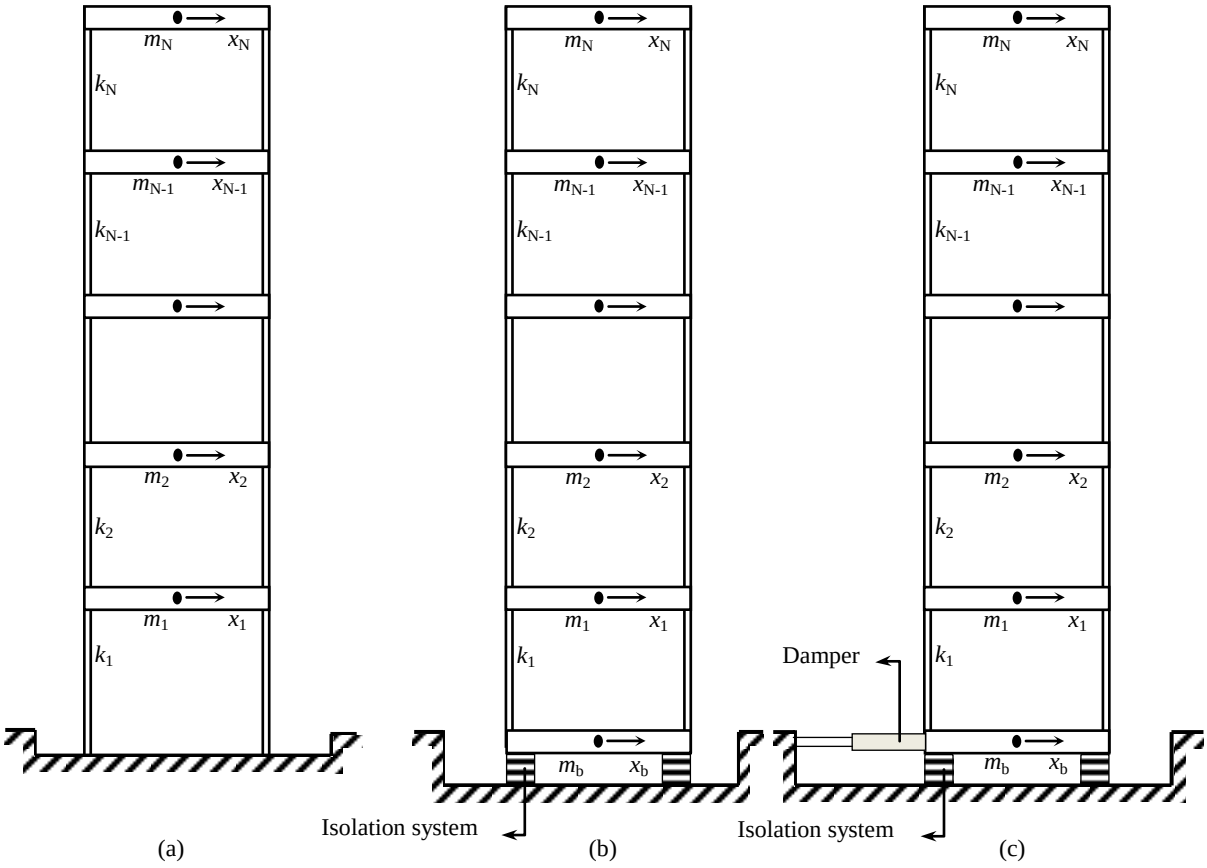

Figure 1: Mathematical models of (a) fixed-base building, (b) base-isolated building, and (c) base-isolated building with supplemental damper.

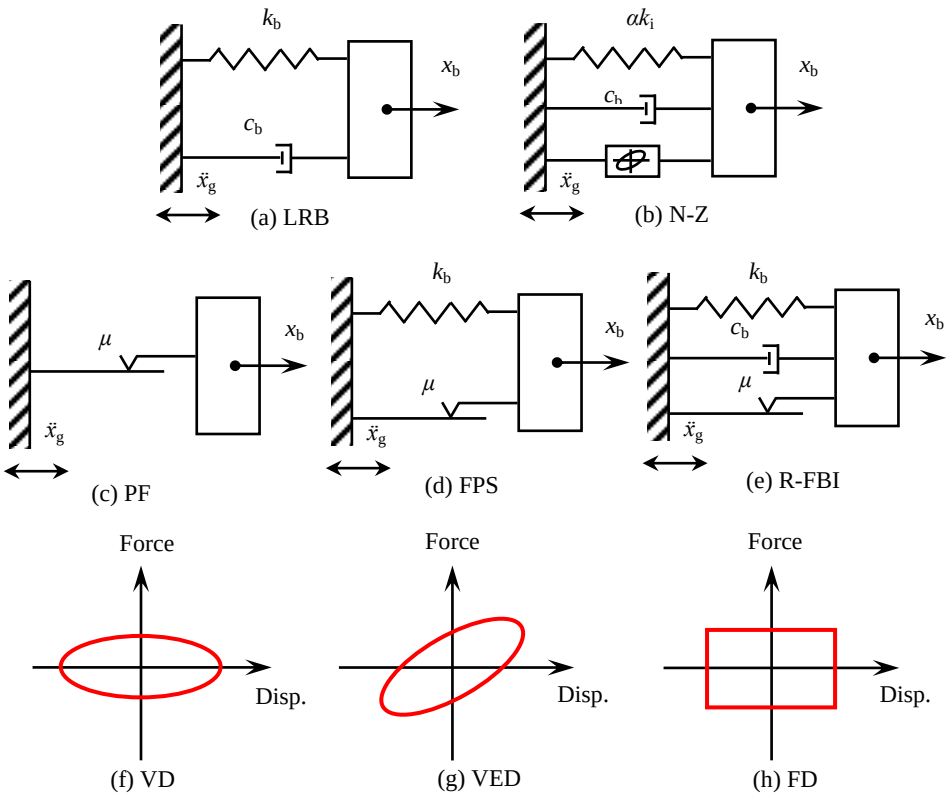

Figure 2: Schematic representations of isolation systems and force-deformation relations for dampers.

Friction Pendulum System (FPS)

The response of friction pendulum system (FPS) depends on the friction coefficient and the geometry of the isolation system [28]. The system becomes active only when the static value of friction is exceeded by the earthquake force. Restoring force is generated in the FPS due to the raising of the structure caused by the concave geometry of the isolator. The total lateral force developed is equal to the sum of restoring and friction forces. The restoring force is given by

$$F_{\mathrm{b}} = k_{\mathrm{b}} x_{\mathrm{b}} + F_{\mathrm{x}} \tag{7}$$

where k_{b} is the bearing stiffness, and $F_{\mathrm{x}} = \mu W$ is the friction force.

The isolation period (T_{b}) and friction coefficient (μ) are the parameters used to characterize the FPS and the stiffness of the isolation system (k_{b}) is selected using Equation 3 so that the required isolation period is obtained. The isolation stiffness here refers the concavity of the FPS.

Resilient-Friction Base Isolator (R-FBI)

Sliding flat ring elements and central rubber core are constituents of resilient-friction base isolator (R-FBI) and the sliding rings are Teflon-coated to reduce friction while flexible cover is used as protection against corrosion and dust [29]. The restoring force in the R-FBI is given by

$$F_{\mathrm{b}} = c_{\mathrm{b}} \dot{x}_{\mathrm{b}} + k_{\mathrm{b}} x_{\mathrm{b}} + F_{\mathrm{x}} . \tag{8}$$

Here, $F_{\mathrm{x}} = \mu W$ is the friction force. The isolation period (T_{b}), friction coefficient (μ), and damping ratio (ξ_{b}) are the parameters used to characterize the R-FBI. The damping coefficient (c_{b}) and the stiffness of the isolation system (k_{b}) are selected respectively using Equations 2 and 3 so that the required damping ratio and isolation period are obtained.

Viscous Damper (VD)

Viscous dampers (VDs) are velocity dependent energy dissipation devices and the damping force generated is directly proportional to the relative velocity between the two ends of the damper. A damping exponent of 1 is used to model the viscous damper in this study and the damping force (F_{d}) generated in the damper is expressed as

$$F_{\mathrm{d}} = c_{\mathrm{d}} \dot{x}_{\mathrm{b}} \tag{9}$$

where $\dot{x}_{\mathrm{b}}$ is the relative velocity between the two ends of the damper, i.e. the relative velocity between the base mass and the ground for this study, and c_{d} is the damping coefficient of the viscous damper. The external damping ratio (ξ_{d}) added to the system due to the supplemental viscous damper is defined as

$$\xi_{\mathrm{d}} = \frac{c_{\mathrm{d}}}{2 m \omega_{\mathrm{b}}} . \tag{10}$$

Viscoelastic Damper (VED)

In viscoelastic dampers (VEDs), energy is dissipated through shear deformation of viscoelastic layer. These dampers are velocity dependent and can be modeled using a spring-dashpot element acting in parallel. The force generated in the VEDs is a combination of damping force and elastic force. The damping force is directly proportional to the relative velocity between the two ends of the damper while the elastic force is proportional to the relative displacement. The force generated in the viscoelastic damper (F_{d}) is expressed as

$$F_{\mathrm{d}} = k_{\mathrm{d}} x_{\mathrm{b}} + c_{\mathrm{d}} \dot{x}_{\mathrm{b}} \tag{11}$$

where k_{d} is the stiffness of the viscoelastic damper. The external damping ratio (ξ_{d}) added to the system due to the supplemental viscoelastic damper can be expressed using Equation 10 while the relative external damper stiffness (k'), expressed in terms of the isolation effective stiffness, is defined as

$$k' = \frac{k_{\mathrm{d}}}{\omega_{\mathrm{b}}^2 m} . \tag{12}$$

Friction Damper (FD)

The force generated in a friction damper (FD) arises from friction. The friction force in the damper has typical Coulomb friction characteristics. The displacement in the damper will occur only if the force induced in the damper reaches the limiting friction force (F_{L}). The FD is represented here using the normalized limiting friction force ($\mu_{\mathrm{d}} = F_{\mathrm{L}}/W$) and the force generated in the damper (F_{d}) is expressed as

$$F_{\mathrm{d}} = \mu_{\mathrm{d}} W \operatorname{sgn}\left(\dot{x}_{\mathrm{b}}\right) . \tag{13}$$

GOVERNING EQUATIONS OF MOTION

The governing equations of motion are derived by taking equilibrium of forces at each degree of freedom during seismic excitation. The equations of motion for the base-isolated building with supplemental damper expressed in the matrix form, which is of order of the number of degrees of freedom in the building (N+1), are given as

$$\begin{bmatrix} m & \boldsymbol{r}^{\mathrm{T}}\boldsymbol{M} \\ \boldsymbol{M}\boldsymbol{r} & \boldsymbol{M} \end{bmatrix} \begin{Bmatrix} \ddot{x}_{\mathrm{b}} \\ \ddot{\boldsymbol{X}} \end{Bmatrix} + \begin{bmatrix} c & \boldsymbol{0} \\ \boldsymbol{0} & \boldsymbol{C} \end{bmatrix} \begin{Bmatrix} \dot{x}_{\mathrm{b}} \\ \dot{\boldsymbol{X}} \end{Bmatrix} + \begin{bmatrix} k & \boldsymbol{0} \\ \boldsymbol{0} & \boldsymbol{K} \end{bmatrix} \begin{Bmatrix} x_{\mathrm{b}} \\ \boldsymbol{X} \end{Bmatrix} = -\begin{bmatrix} m & \boldsymbol{r}^{\mathrm{T}}\boldsymbol{M} \\ \boldsymbol{M}\boldsymbol{r} & \boldsymbol{M} \end{bmatrix} \begin{Bmatrix} 1 \\ \boldsymbol{0} \end{Bmatrix} \ddot{x}_{\mathrm{g}} \tag{14}$$

where $\boldsymbol{M} = \operatorname{diag}\left[m_1, m_2, \ldots, m_{\mathrm{N}}\right]$, $\boldsymbol{C}$, and $\boldsymbol{K}$ are the mass, damping, and stiffness matrices of the superstructure which are of order $(N \times N)$, respectively; c and k are respectively the damping coefficient and stiffness at the isolation level obtained by combining the contributions of the isolator and attached damper; x_{b}, $\dot{x}_{\mathrm{b}}$, and $\ddot{x}_{\mathrm{b}}$ are the displacement, velocity, and acceleration of the base mass relative to the ground, respectively; $\boldsymbol{X} = \left\{x_1, x_2, \ldots, x_{\mathrm{N}}\right\}^{\mathrm{T}}$, $\dot{\boldsymbol{X}}$, and $\ddot{\boldsymbol{X}}$ are the vectors of floor displacements, velocities, and accelerations, respectively, relative to the base mass; $\boldsymbol{r} = \{\boldsymbol{1}\}$ is vector of influence coefficients; and $\ddot{x}_{\mathrm{g}}$ is the earthquake ground acceleration.

Due to the non-linear force-deformation behavior of the isolator and the difference between the damping of the isolation system, the superstructure, and the supplemental damper, the equations of motion cannot be solved using the classical modal superposition technique. Therefore, the equations of motion are numerically solved using the Newmark's method of step-by-step integration using a small time interval (Δt) with linear variation of acceleration.

NUMERICAL STUDY

The effect of viscous, viscoelastic, and friction supplemental dampers on the response of base-isolated building is studied here. Multi-storey shear model of a building is used in the investigation and the supplemental damper is connected at the isolation level with one end attached to the ground and the other to the base mass.

The seismic response of five-storey building models are investigated under real earthquake ground motion records.

Three near-fault (NF) and three far-fault (FF) ground motions with varying Richter scale magnitudes are used for the study. The peak ground accelerations (PGAs) and other relevant details of the selected ground motion data are shown in Table 1.

Base Isolation Systems

Laminated rubber bearing is modeled using isolation period (T_b) and damping ratio (ξ_b) while N-Z system is modeled using isolation period (T_b), damping ratio (ξ_b), normalized yield strength (F_o) and isolator yield displacement (q). Friction coefficient (μ) is used to characterize the PF system and FPS; with FPS having stiffness (k_b) in addition to the friction coefficient. The R-FBI system is modeled using similar parameters as that for the FPS with additional damping parameter (ξ_b) incorporated.

Throughout this study, a five-storey building with fundamental fixed-base time period (T) of 0.5 sec is investigated. The five isolation systems are modeled with specific parameters and paired with the three types of dampers and the response are compared. In this study, ξ_b values of 0.1, 0.15, 0.2, and 0.25; T_b values of 1.5, 1.75, 2, 2.25, 2.5, 2.75, and 3 sec; F_o and μ values of 0.05, 0.075, 0.1, 0.125 and 0.15; and q of 2.5 cm are used to model the five isolation systems accordingly.

Effect of Viscous Damper

Viscous damper is velocity dependent damping device and the parameter used in modeling includes the damping coefficient (c_d) which is obtained using Equation 10 in terms of the external damping ratio (ξ_d) added to the system. For this study, ξ_d values of 5%, 10%, 15%, 20%, 25%, 30%, 35% and 40% are considered.

The time histories of top floor acceleration, isolator displacement, and storey shear for the five-storied base-isolated building with the R-FBI and viscous damper under the 1989 Loma Prieta, the 1994 Northridge, and the 1995 Kobe ground motions are plotted in Figure 3.

The influence of the external damping (ξ_d) added to the system on the responses of the base-isolated building is investigated and the trend is obtained for each isolation system. Figure 4 shows the trend of the influence of ξ_d on the response of a building isolated by the R-FBI under near-fault ground motions. To derive a generalized trend, the average of the patterns for all isolation systems is obtained and plotted together in Figures 5 and 6 for near-fault and far-fault ground motions, respectively. These plots show that the increase in the damping ratio of the damper (ξ_d) causes the isolator displacement to reduce and the top floor acceleration to increase marginally. As ξ_d increases, the normalized first storey shear decreases initially and then show increment after certain damping is reached. It is observed that minimum storey shear values are achieved for certain range of the damping ratio of the damper (ξ_d).

Effect of Viscoelastic Damper

The force-displacement model of viscoelastic damper is represented with combined effect of the damper elastic force and the damping force. The elastic force is represented with the damper stiffness (k_d) which can be obtained from the relative external damper stiffness (k') while damping coefficient of damper (c_d) is used to obtain the damping force. Here, c_d is expressed in terms of the external damping (ξ_d) added to the system due to the supplemental viscoelastic device. Relative external damper stiffness values of 0.05, 0.15, 0.3, 0.5, 0.75, 1.1, 1.5 and 2 are used while the damping coefficient values considered here are same as that of the viscous dampers.

Figure 3 also shows the time histories of top floor acceleration, isolator displacement, and storey shear for the five-storied base-isolated building modeled using the R-FBI with viscoelastic damper under the 1989 Loma Prieta, the 1994 Northridge, and the 1995 Kobe ground motions.

The influence of the external damping (ξ_d) and the relative damper stiffness (k') added to the system on the response of the base-isolated building are investigated and the trends can be observed from Figures 5 and 6. The general trend shows that the increase in the damping ratio of the damper (ξ_d) causes the isolator displacement to reduce while the top floor acceleration and normalized first storey shear increase marginally.

The increase in the k' reduces the isolator displacement while the top floor acceleration and first storey shear generally increase initially however then start to reduce after a certain value of the k'.

Effect of Friction Damper

Friction dampers are displacement dependent devices and are modeled in this study by specifying the limiting friction force (F_L). The normalized limiting friction force ($\mu_d = F_L/W$), which is the ratio of the limiting friction force to the total weight of the base-isolated building, is used to define the friction damper. Values of μ_d used are 0.015, 0.03, 0.05, 0.07, 0.09, 0.11, 0.13, 0.15, 0.17, 0.19, 0.21, 0.23 and 0.25.

The time histories of the response for the five-storied base-isolated building with the R-FBI and the three types of dampers considered here under the three near-fault ground motions are shown in Figure 3.

Table 1: List of near-fault and far-fault earthquake ground motions used in the study.

No.	Earthquake Name	Year	Station Name	Magnitude	PGA (g)	NF/FF
1	Loma Prieta, USA	1989	Los Gatos Presentation Center (LGPC)	6.93	0.97	NF
2	Northridge, USA	1994	Sylmar - Hospital	6.69	0.84	NF
3	Kobe, Japan	1995	Kobe Japan Meteorological Agency (KJMA)	6.90	0.83	NF
4	Imperial Valley, USA	1940	El Centro Array #9-117	7.0	0.27	FF
5	Tabas, Iran	1978	Ferdows	7.4	0.26	FF
6	Northridge, USA	1994	Century City CC North	6.7	0.11	FF

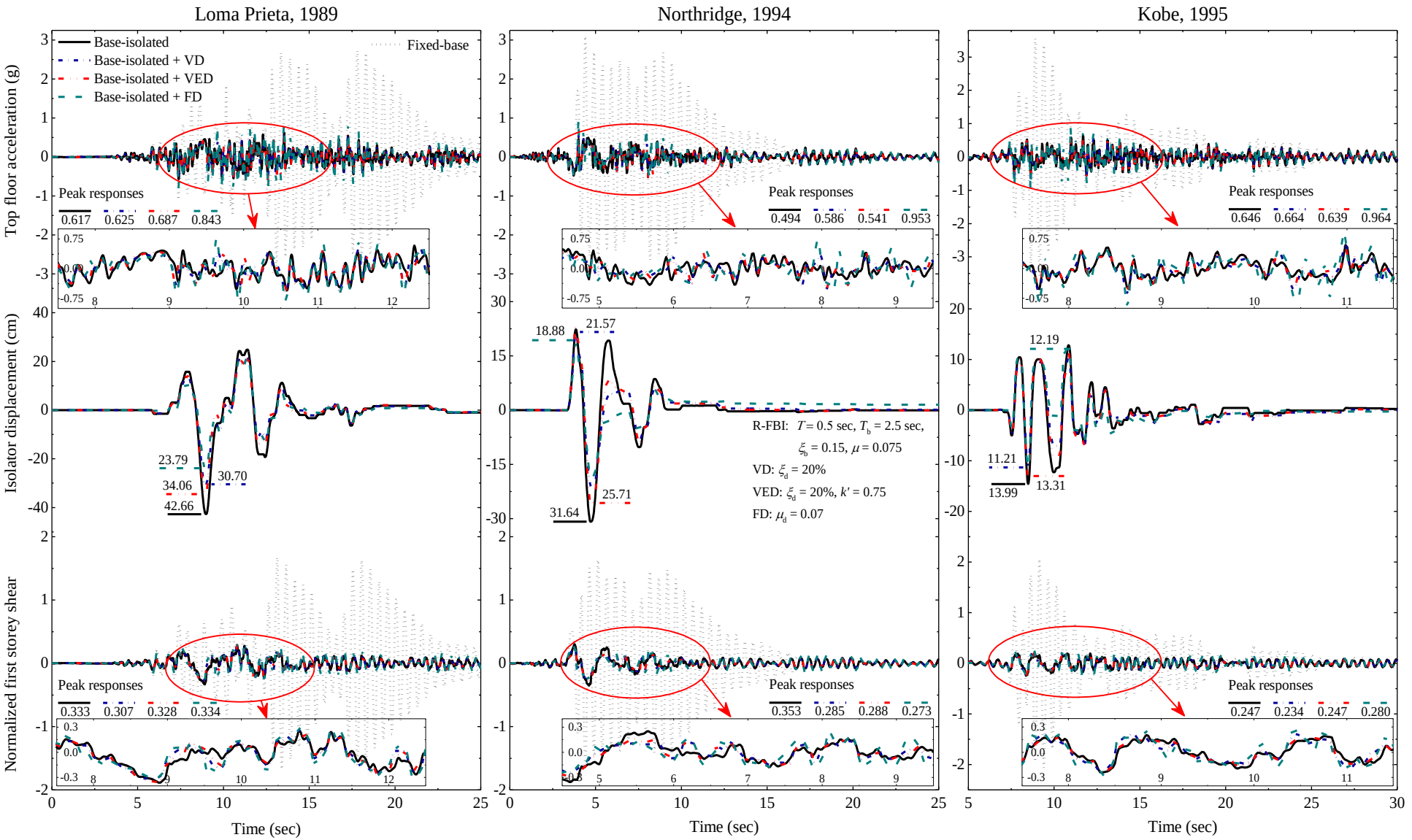

Figure 3:Time histories of isolator displacement, top floor acceleration, and normalized first storey shear of five-storey building isolated by R-FBI under near-fault ground motions.

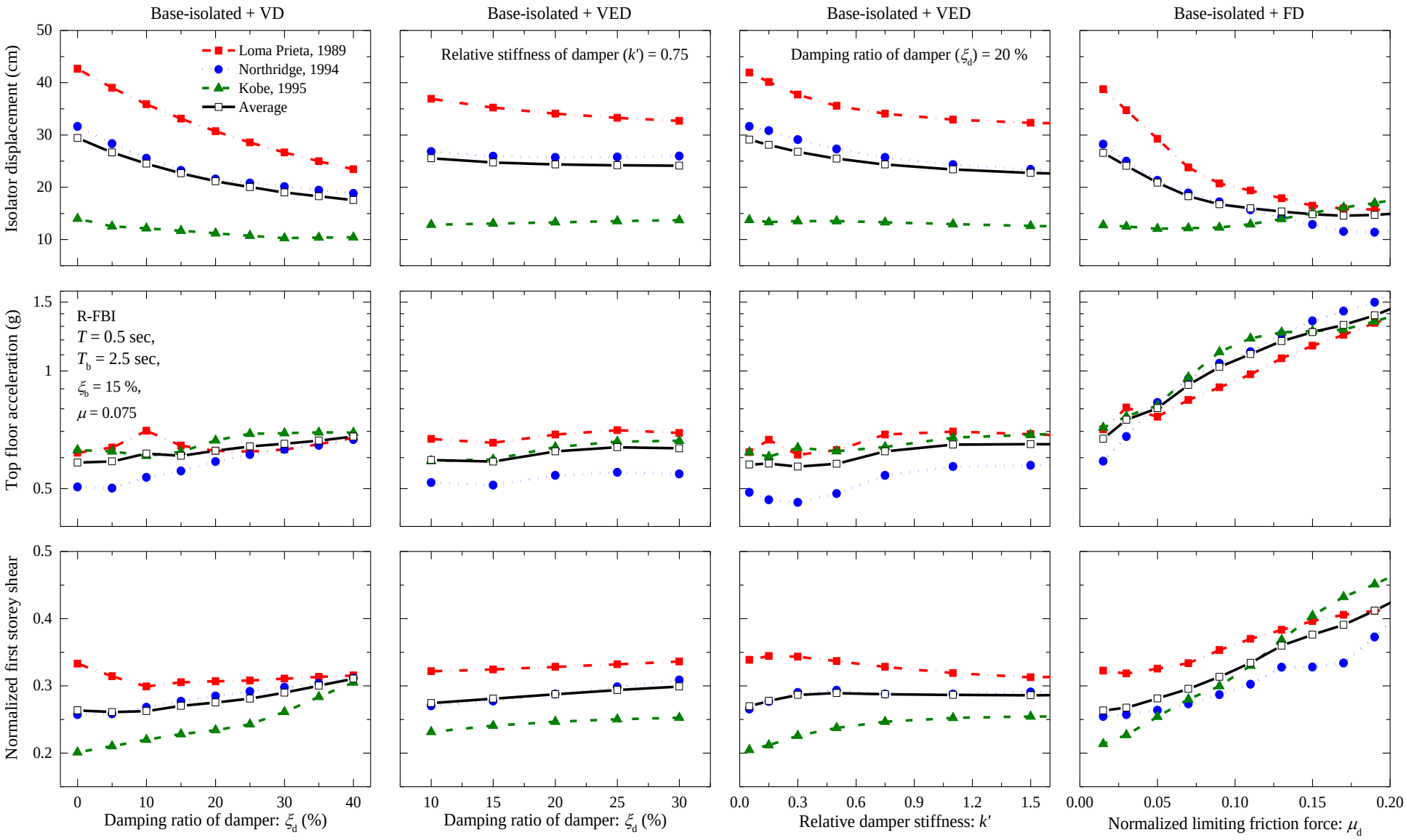

Figure 4: Effect of damper parameters on the responses of five-storey building isolated by R-FBI under near-fault ground motions (T = 0.5 sec, T_b = 2.5 sec, μ = 0.075, ξ_b = 15%).

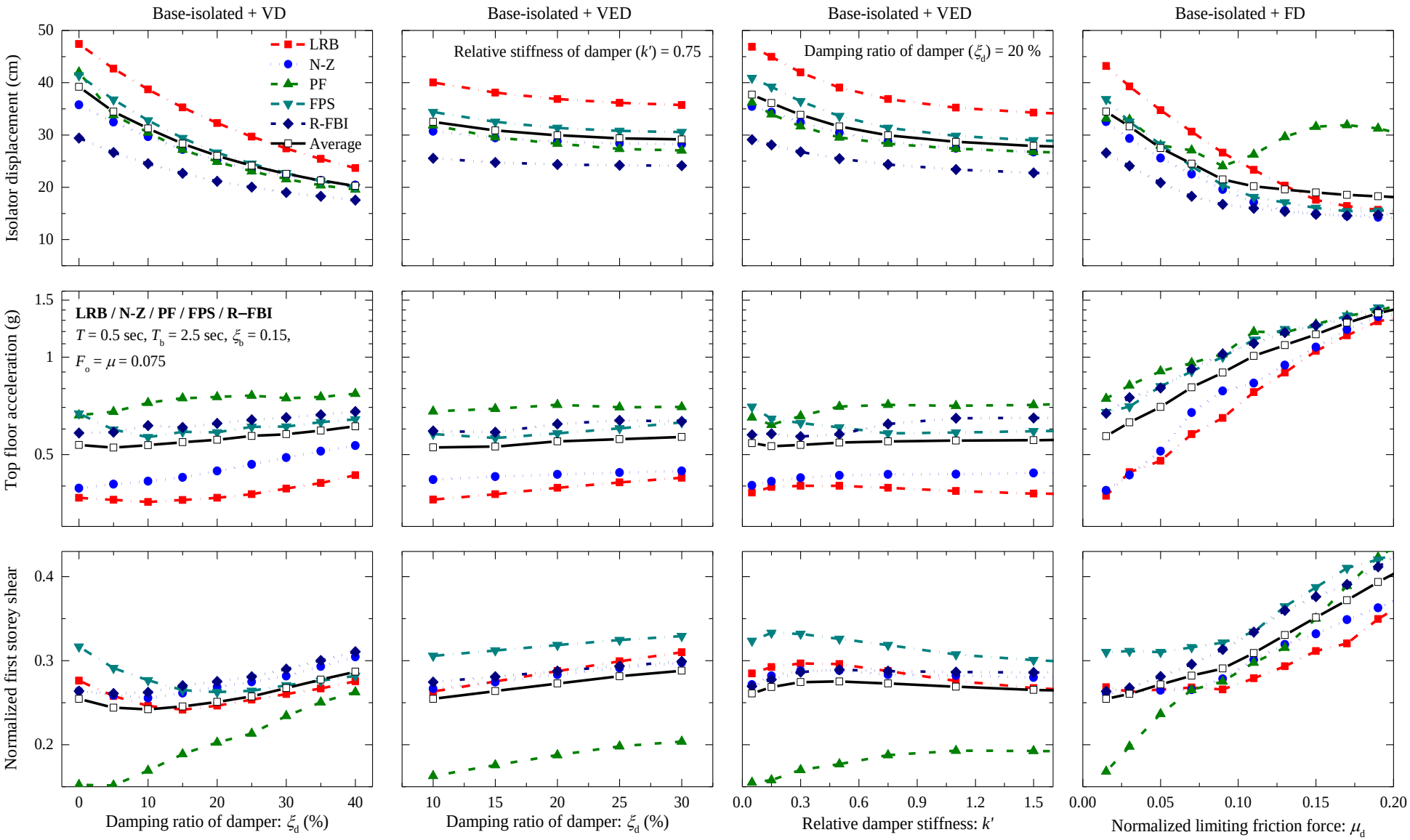

Figure 5: Effect of damper parameters on the responses of five-storey base-isolated building isolated by all five base isolation systems under near-fault ground motions (T = 0.5 sec, T_b = 2.5 sec).

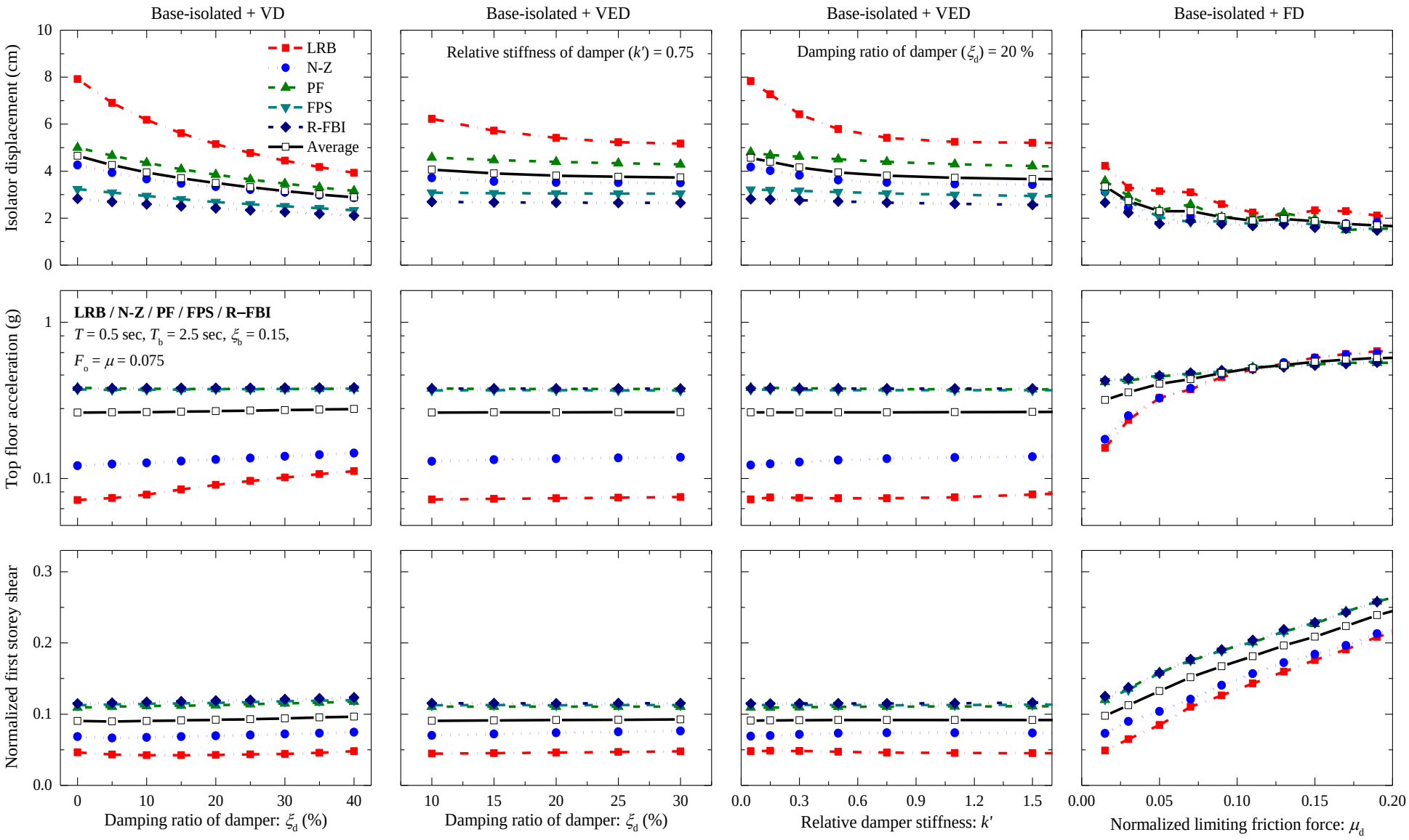

Figure 6: Effect of damper parameters on the responses of five-storey base-isolated building isolated by all the five isolation systems under far-fault ground motions (T = 0.5 sec, T_b = 2.5 sec).

The influence of the limiting friction force (μ_d) on the responses of the base-isolated building is investigated and the trend is plotted in Figures 5 and 6. These plots show that the increase in the limiting friction force (μ_d) causes the isolator displacement to reduce significantly for certain values of μ_d and the rate of reduction of the isolator displacement reduces afterwards for all isolators except for the PF system. For the PF system, the isolator displacement reduces initially and then starts to increase after some value of μ_d is reached because of the introduction of the large slip load to the system. The top floor acceleration and normalized first storey shear keep increasing for an increase in μ_d; however, the rate of increment is smaller initially and becomes larger for higher values of the μ_d. The increase in the top floor acceleration and the first storey shear is mainly caused due to the large initial stiffness of the FD which also increases the acceleration associated with higher frequencies.

The peak responses of a base-isolated building with the VD, VED, and FD of selected parameters are shown in Table 2. It is seen that the isolator displacement is significantly reduced when VD, VED, and FD are used.

Study of Responses for Various Dampers and Isolation Systems

Figure 7 shows the force-deformation behavior of the R-FBI and dampers for the base-isolated building as well as base-isolated buildings with the supplemental dampers under the three near-fault ground motions. Comparison of the plots of each model with supplemental damper to that without the damper clearly shows that the use of all the three supplemental dampers is helpful in reducing the isolator displacement. The force-deformation relations also indicate the relative effectiveness of the viscous, viscoelastic, and friction dampers showing that the friction damper and viscous damper are more effective in reducing deformation at the isolator level.

Figure 8 shows, in addition to the effectiveness of the dampers in reducing the bearing displacement, the distribution of the peak floor displacement, peak floor acceleration, and peak storey shear over the total height of the building. The plots of floor accelerations and the normalized storey shear show that these responses are not undesirably affected, due to the use of the supplemental dampers, throughout the height of the building. The application of the friction damper caused the largest increment in the acceleration response; however, the response remained well below the case of the fixed-base building. The plots of the floor displacements also show decrease in the peak lateral displacement of the building at all floor levels due to the application of the supplemental dampers. This indicates that the supplemental dampers can also be helpful in minimizing the risk of pounding in base-isolated buildings. Such use of dampers for minimizing the risk of pounding at superstructure level connecting adjacent buildings in case of the base-isolated building was established earlier [30].

In Figure 9, the comparison of the FFT amplitude spectra of top floor acceleration for the base-isolated building and base-isolated building with each damper type is shown. The FFT spectra of top floor acceleration obtained for the base-isolated building with the VD and VED are relatively not significantly different from that of the base-isolated building without supplemental damper. However, the Fourier spectra for the base-isolated building fitted with the FD is significantly different and indicates that there is high contribution in the superstructure acceleration from high frequencies. This is caused due to the high initial stiffness of the friction damper introduced to the system, which is suddenly changed to low stiffness, inducing sudden change of phase from stick to slip and vice-versa. The large acceleration in the superstructure associated with high frequencies is undesirable for sensitive equipment and secondary structures in the building. This is because of the occurrence of resonant effect in the sensitive equipment and secondary structures in the building which usually vibrate in the same frequency range. Hence, performance of the FD is inferior as compared to the VD and VED from this viewpoint.

The time histories of input and dissipated energies per unit mass (E) of the base-isolated building with and without supplemental damper are shown in Figure 10. The energy plots show that the supplemental dampers dissipate significant amount of the earthquake energy. A comparison between the three types of dampers also shows that the FD dissipates the highest amount of energy followed by the viscous damper. The plots also show that the energy dissipated by the base-isolator is lower when a damper is used which dissipates higher amount of energy.

Based on the peak responses of the base-isolated building presented in Table 2, the percentage reductions of the responses under the three near-fault ground motion considered are determined and shown in Table 3.

The plots of the peak isolator displacement, top floor acceleration, and normalized first-storey shear, shown in Figure 11, indicate the effectiveness of each of the combinations of isolation system and damper explored in reducing the isolator displacement without adversely affecting the top floor acceleration and the storey shear. It is observed that installing the FD results in the largest reduction in isolator displacement for all isolation systems except when the PF isolation system is used. However, both the top floor acceleration and normalized storey shear are found to be high when the FD is used. Although the top floor accelerations obtained for base-isolated building models with the VED are low, the isolator displacement obtained is large as compared to that of the VD and FD. The storey shear is also higher relative to the case of base-isolated buildings with the VD. The isolator displacement obtained when viscous dampers are used is marginally higher in comparison with the case where FDs are used. However, the VD has advantages over the FD in giving lower floor acceleration and storey shear. From the five isolation systems considered, the R-FBI results in the lowest isolator displacement followed by the N-Z system with all three damper types. The LRB is observed to exhibit the largest isolator displacement while the PF system and FPS result in moderate isolator displacement. The PF system and FD are also apparently resulting in large residual isolator displacements due to absence of restoring force, which hence is undesirable combination. Thus, the combination of the R-FBI and VD is recommended for achieving maximum isolator displacement reduction.

Figure 12 shows the effect of isolation period (T_b) on the percentage reduction in the responses of five-storey base-isolated building with supplemental dampers. It is observed that T_b does not have significant effect on the percentage reduction in the isolator displacement of base-isolated building with the VD. However, the increase in T_b causes lesser and higher percentage reduction of isolator displacement for base-isolated building with the VED and FD, respectively. Although base-isolated building with the FD having large T_b benefits from higher percentage reduction in isolator displacement, top floor acceleration, and storey shear show larger increase. The percentage reduction in top floor acceleration of base-isolated building with the VD and VED does not vary significantly with the T_b while increase in the T_b causes lesser control of the first storey shear.

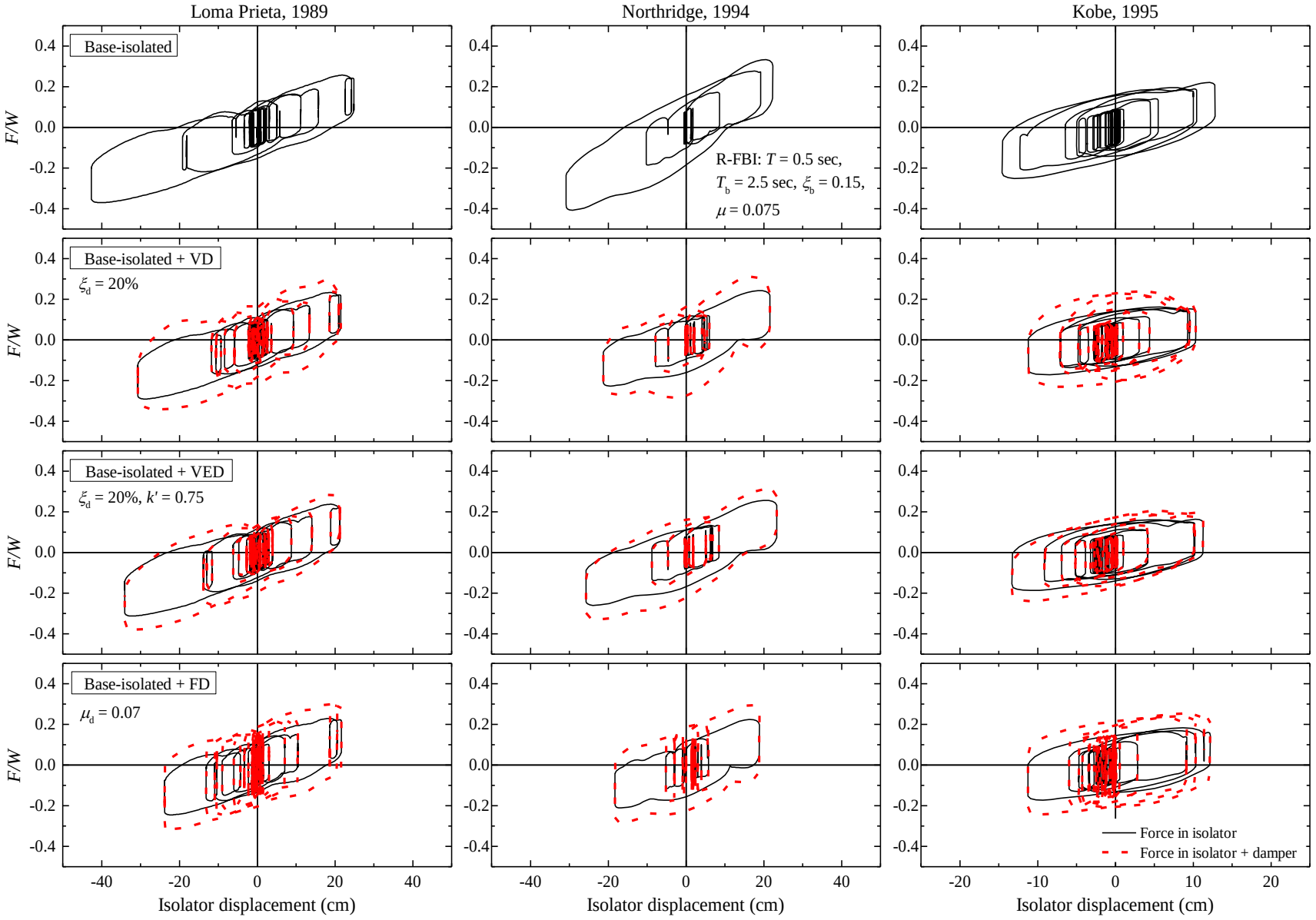

Figure 7: Comparison of force-deformation behavior of isolator for five-storey building isolated by R-FBI with and without supplemental dampers under near-fault ground motions.

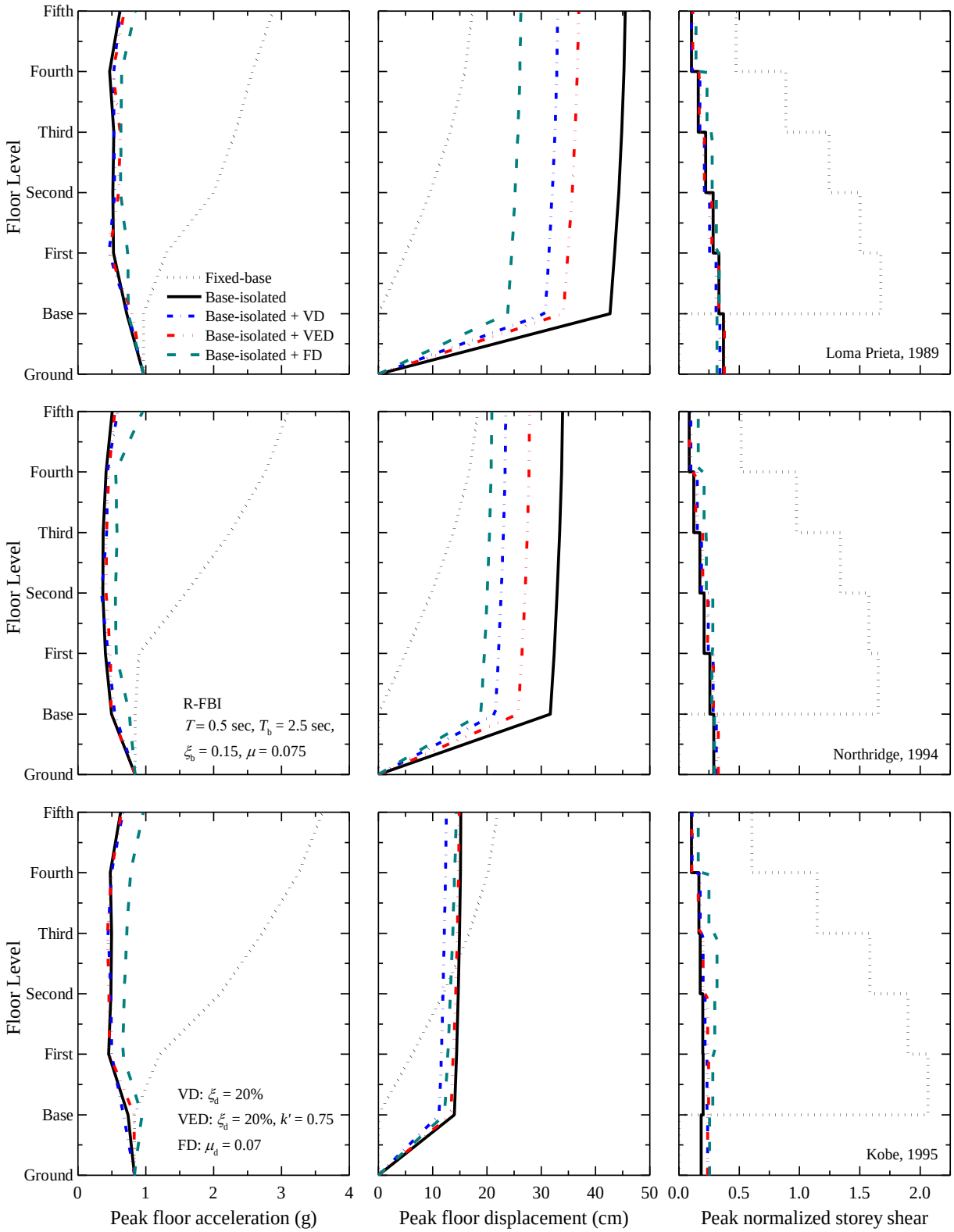

Figure 8: Distribution of peak floor acceleration, peak floor displacement, and peak normalized storey shear over the height of five-storey base-isolated building under near-fault ground motions.

Table 2: Peak responses of five-storey base-isolated building with and without supplemental damper under near-fault ground motions (T = 0.5 sec, T_b = 2.5 sec).

Response under near-fault ground motions			Base-isolated	Base-isolated building with			Fixed-base
				VD (ξ_d = 20%)	VED (ξ_d = 20%, k' = 0.75)	FD (μ_d = 0.07)	
LRB ξ_b = 0.15 T_b = 2.5 sec	Loma Prieta, 1989	Isolator displacement (cm)	64.558	44.902	50.457	43.990	-
		Top floor acceleration (g)	0.476	0.421	0.466	0.650	2.875
		Normalized first storey shear	0.376	0.322	0.376	0.335	1.675
	Northridge, 1994	Isolator displacement (cm)	49.227	32.972	38.633	32.981	-
		Top floor acceleration (g)	0.396	0.368	0.404	0.463	3.098
		Normalized first storey shear	0.284	0.259	0.301	0.266	1.652
	Kobe, 1995	Isolator displacement (cm)	28.378	18.975	21.518	14.921	-
		Top floor acceleration (g)	0.231	0.315	0.314	0.621	3.606
		Normalized first storey shear	0.168	0.158	0.186	0.203	2.066
N-Z ξ_b = 0.15, F_o = 0.075, q = 2.5 cm, T_b = 2.5 sec	Loma Prieta, 1989	Isolator displacement (cm)	48.231	35.776	39.049	30.667	-
		Top floor acceleration (g)	0.438	0.421	0.461	0.776	2.875
		Normalized first storey shear	0.324	0.305	0.336	0.298	1.675
	Northridge, 1994	Isolator displacement (cm)	37.986	25.421	30.334	23.703	-
		Top floor acceleration (g)	0.395	0.456	0.459	0.525	3.098
		Normalized first storey shear	0.268	0.276	0.308	0.271	1.652
	Kobe, 1995	Isolator displacement (cm)	21.128	14.169	16.878	13.257	-
		Top floor acceleration (g)	0.348	0.456	0.382	0.723	3.606
		Normalized first storey shear	0.199	0.224	0.206	0.228	2.066
PF μ = 0.075	Loma Prieta, 1989	Isolator displacement (cm)	65.724	32.059	39.066	32.410	-
		Top floor acceleration (g)	0.675	0.591	0.617	0.829	2.875
		Normalized first storey shear	0.155	0.170	0.179	0.237	1.675
	Northridge, 1994	Isolator displacement (cm)	42.459	29.864	33.987	26.191	-
		Top floor acceleration (g)	0.637	0.926	0.873	1.001	3.098
		Normalized first storey shear	0.160	0.239	0.198	0.307	1.652
	Kobe, 1995	Isolator displacement (cm)	17.814	16.450	17.188	22.683	-
		Top floor acceleration (g)	0.676	0.730	0.658	1.048	3.606
		Normalized first storey shear	0.142	0.183	0.175	0.252	2.066
FPS μ = 0.075, T_b = 2.5 sec	Loma Prieta, 1989	Isolator displacement (cm)	57.127	39.016	44.121	32.877	-
		Top floor acceleration (g)	0.705	0.631	0.638	0.900	2.875
		Normalized first storey shear	0.414	0.315	0.399	0.343	1.675
	Northridge, 1994	Isolator displacement (cm)	45.650	28.314	34.924	24.930	-
		Top floor acceleration (g)	0.591	0.508	0.507	0.860	3.098
		Normalized first storey shear	0.324	0.260	0.327	0.320	1.652
	Kobe, 1995	Isolator displacement (cm)	21.434	12.583	15.075	14.221	-
		Top floor acceleration (g)	0.712	0.619	0.599	0.950	3.606
		Normalized first storey shear	0.212	0.212	0.230	0.285	2.066
R-FBI μ = 0.075, ξ_b = 0.15, T_b = 2.5 sec	Loma Prieta, 1989	Isolator displacement (cm)	42.662	30.705	34.064	23.790	-
		Top floor acceleration (g)	0.617	0.625	0.687	0.843	2.875
		Normalized first storey shear	0.333	0.307	0.328	0.334	1.675
	Northridge, 1994	Isolator displacement (cm)	31.644	21.569	25.706	18.884	-
		Top floor acceleration (g)	0.505	0.586	0.541	0.953	3.098
		Normalized first storey shear	0.257	0.285	0.288	0.273	1.652
	Kobe, 1995	Isolator displacement (cm)	13.989	11.206	13.310	12.189	-
		Top floor acceleration (g)	0.627	0.664	0.639	0.964	3.606
		Normalized first storey shear	0.201	0.234	0.247	0.280	2.066

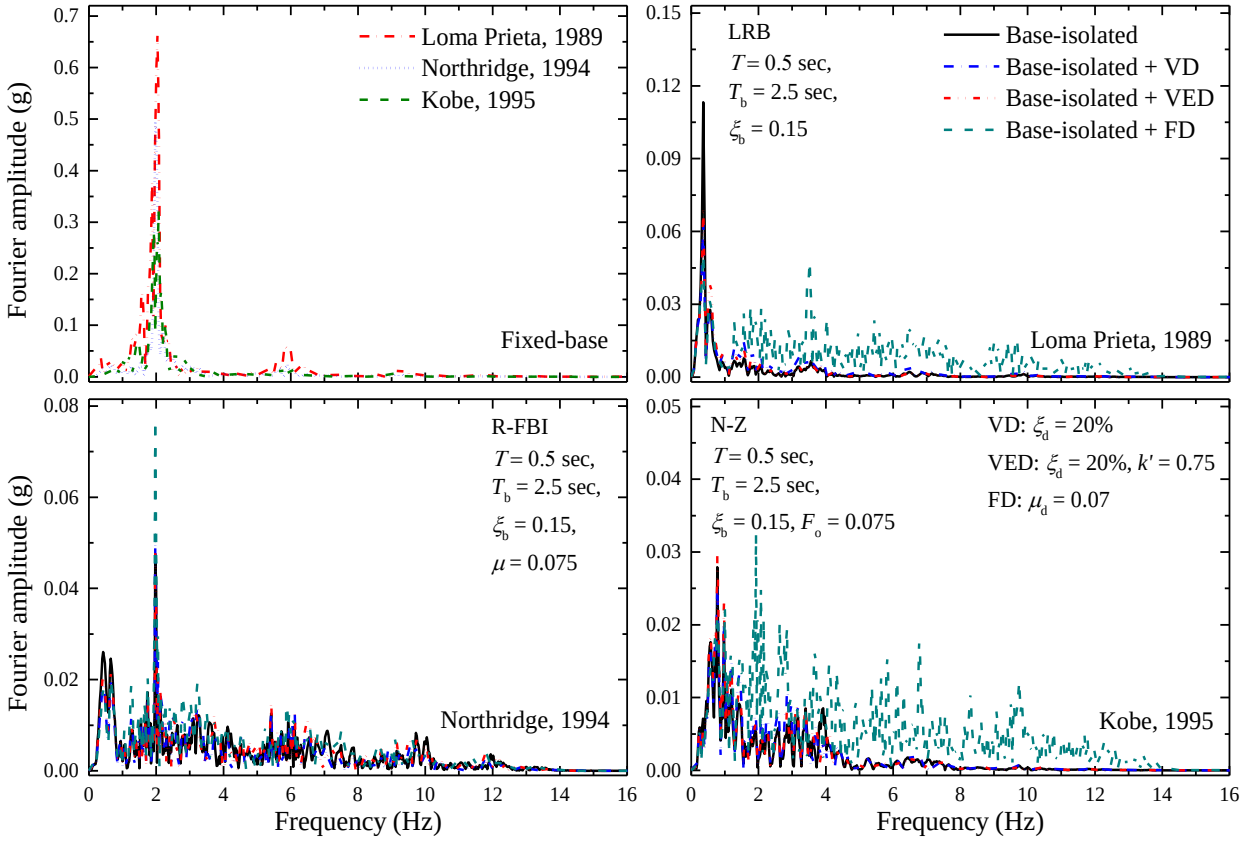

Figure 9: FFT spectra of top floor acceleration for five-storey base-isolated building with and without supplemental dampers under near-fault ground motions.

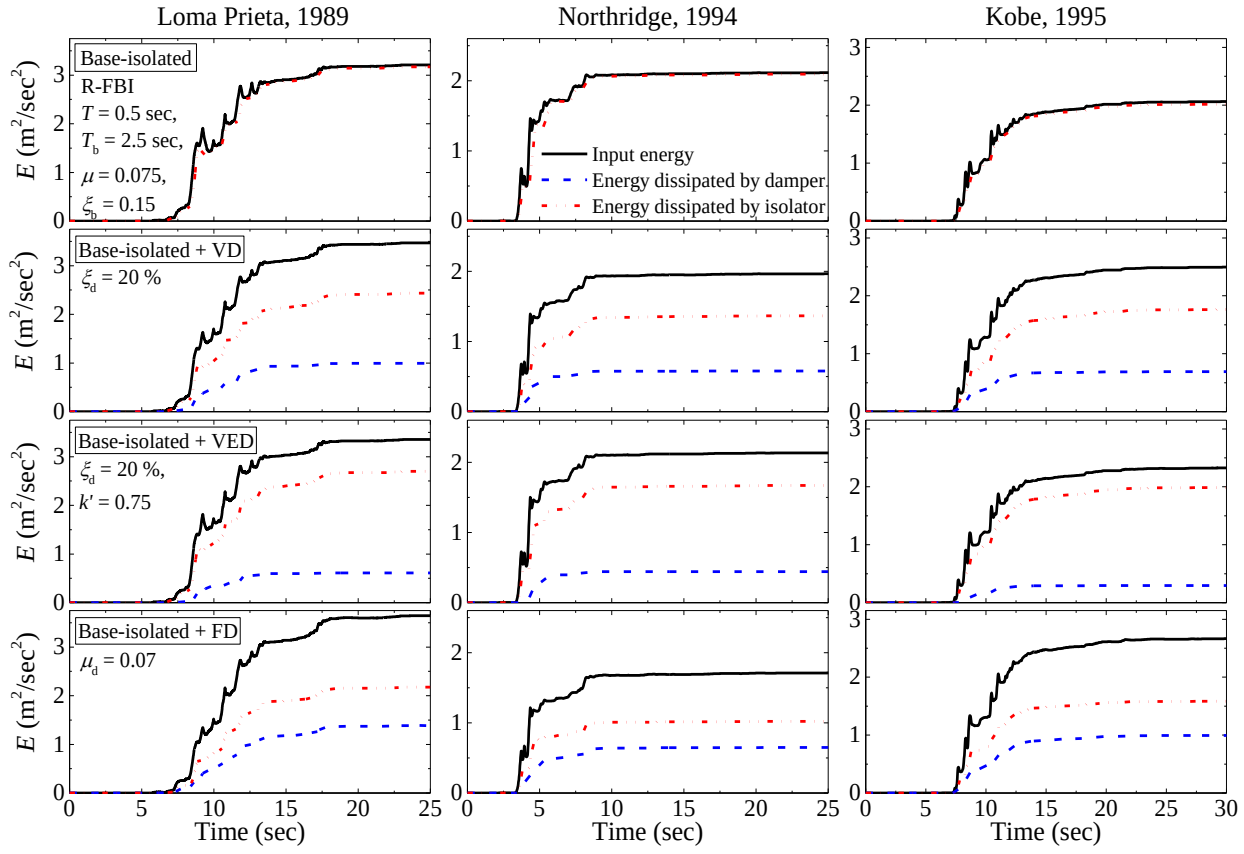

Figure 10: Time histories of input and dissipated energies per unit mass for base-isolated building with and without supplemental dampers.

Table 3: Average percentage reductions in responses of five-storey base-isolated building due to application of supplemental viscous, viscoelastic, and friction dampers under near-fault ground motions (T = 0.5 sec).

Response reduction under near-fault ground motions			Base-isolated building with		
			VD (ξ_d = 20%)	**VED (ξ_d = 20%, k' = 0.75)**	**FD (μ_d = 0.07)**
LRB ξ_b = 0.15	T_b = 2 sec	Isolator displacement (%)	33.590	23.710	34.616
		Top floor acceleration (%)	7.402	2.924	-23.282
		Normalized first storey shear (%)	17.236	4.216	11.592
	T_b = 2.5 sec	Isolator displacement (%)	32.201	22.512	37.428
		Top floor acceleration (%)	-5.882	-11.935	-74.076
		Normalized first storey shear (%)	9.692	-5.486	-1.114
	T_b = 3 sec	Isolator displacement (%)	29.381	16.239	37.202
		Top floor acceleration (%)	-13.034	-8.928	-127.793
		Normalized first storey shear (%)	1.461	-8.460	-14.636
N-Z ξ_b = 0.15, F_o = 0.075, q = 2.5 cm	T_b = 2 sec	Isolator displacement (%)	31.978	23.915	32.808
		Top floor acceleration (%)	-5.745	-3.994	-40.524
		Normalized first storey shear (%)	4.144	-2.883	5.519
	T_b = 2.5 sec	Isolator displacement (%)	30.613	19.766	37.089
		Top floor acceleration (%)	-14.266	-10.474	-72.544
		Normalized first storey shear (%)	-3.192	-7.361	-2.413
	T_b = 3 sec	Isolator displacement (%)	27.894	15.521	38.139
		Top floor acceleration (%)	-13.824	-9.693	-85.736
		Normalized first storey shear (%)	-11.217	-12.383	-14.166
PF μ = 0.075	T_b = 2 sec	Isolator displacement (%)	32.794	24.136	20.556
		Top floor acceleration (%)	-14.983	-0.678	-45.078
		Normalized first storey shear (%)	-36.673	-30.803	-74.207
	T_b = 2.5 sec	Isolator displacement (%)	29.515	21.343	20.556
		Top floor acceleration (%)	-13.668	-8.610	-45.078
		Normalized first storey shear (%)	-29.426	-20.844	-74.207
	T_b = 3 sec	Isolator displacement (%)	27.268	19.564	20.556
		Top floor acceleration (%)	-12.424	-1.628	-45.078
		Normalized first storey shear (%)	-25.779	-12.012	-74.207
FPS μ = 0.075	T_b = 2 sec	Isolator displacement (%)	35.883	25.413	34.199
		Top floor acceleration (%)	16.287	5.819	-18.678
		Normalized first storey shear (%)	16.934	2.325	6.708
	T_b = 2.5 sec	Isolator displacement (%)	36.991	25.310	40.497
		Top floor acceleration (%)	12.573	13.190	-35.562
		Normalized first storey shear (%)	14.444	-1.950	-5.356
	T_b = 3 sec	Isolator displacement (%)	29.322	13.939	33.578
		Top floor acceleration (%)	-14.373	-1.547	-56.506
		Normalized first storey shear (%)	7.215	-10.914	-17.498
R-FBI μ = 0.075, ξ_b = 0.15	T_b = 2 sec	Isolator displacement (%)	26.898	15.782	31.705
		Top floor acceleration (%)	-11.873	-7.875	-58.987
		Normalized first storey shear (%)	2.331	-6.766	-1.997
	T_b = 2.5 sec	Isolator displacement (%)	26.587	14.589	32.475
		Top floor acceleration (%)	-7.741	-6.785	-59.744
		Normalized first storey shear (%)	-6.411	-11.024	-15.224
	T_b = 3 sec	Isolator displacement (%)	22.790	14.014	28.348
		Top floor acceleration (%)	2.424	3.988	-50.617
		Normalized first storey shear (%)	-8.248	-13.561	-24.513

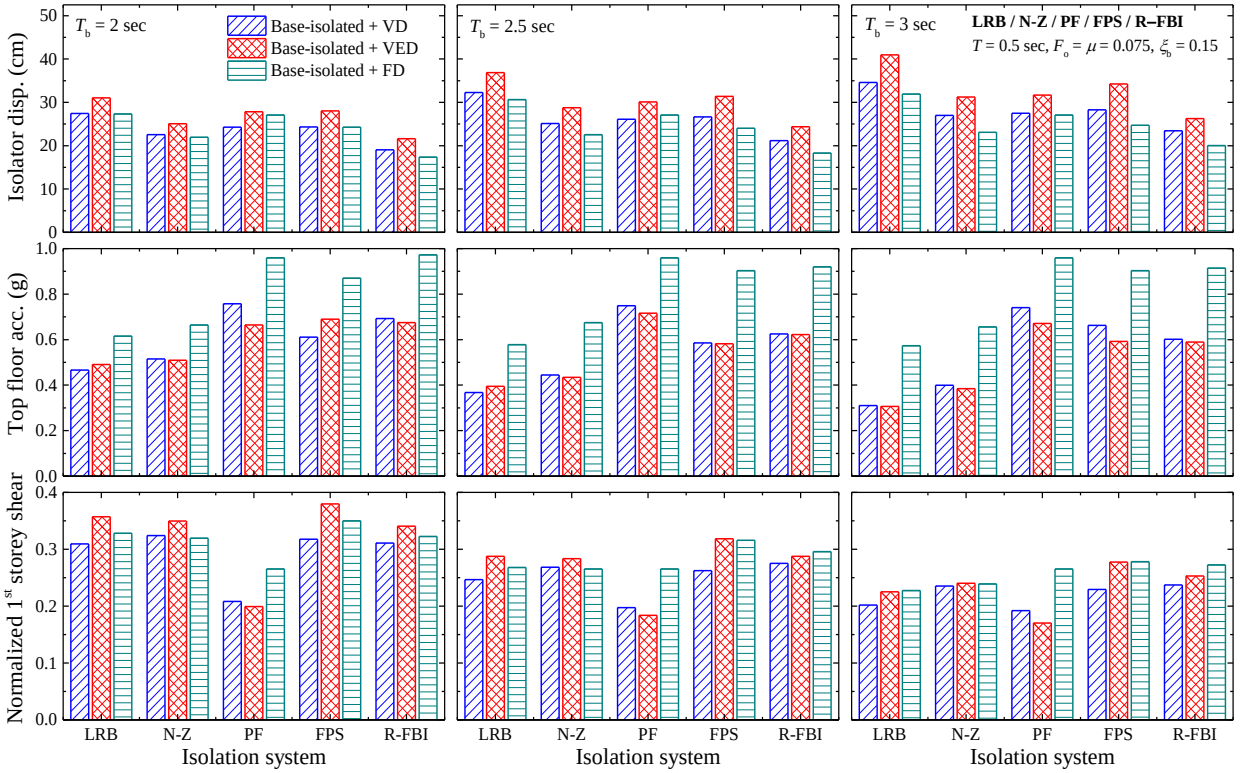

Figure 11: Comparison of the isolator displacement, top floor acceleration, and normalized first storey shear achieved for the combinations of isolators and dampers under near-fault ground motions.

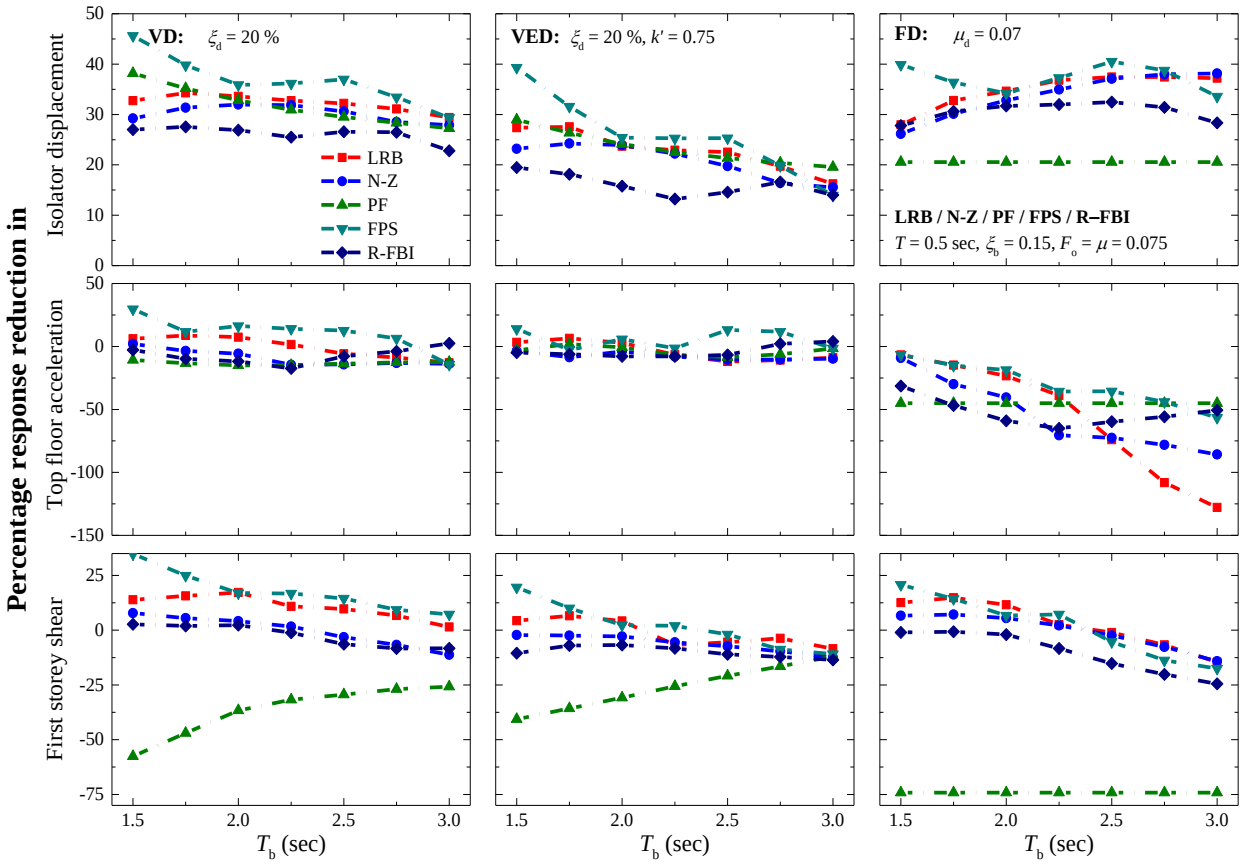

Figure 12: Effect of isolation period on the percentage reduction in responses of five-storey base-isolated building with supplemental dampers under near-fault ground motions.

Responses under Near-Fault and Far-Fault Ground Motions

Comparison of the responses of the base-isolated building with supplemental dampers under near-fault and far-fault ground motions show that near-fault ground motions result in larger response irrespective of providing the isolation and damping system. The trends in Figures 5 and 6 also indicate that base-isolated buildings subjected to the near-fault excitations benefit substantially from the supplemental damping devices provided.

CONCLUSIONS

In this study, the effect of viscous, viscoelastic, and friction supplemental dampers on the seismic response of base-isolated buildings with various isolation systems is investigated. The influence of installing the supplemental dampers on isolator displacement, floor acceleration, and storey shear of base-isolated building is investigated. Parametric study is conducted to arrive at range of parameters for optimum responses and the effectiveness of each of the dampers in reducing the isolator displacement without affecting other responses to undesirable extent is quantified. Finally, the contributions of all the isolator and damper combinations in controlling the seismic response of the base-isolated building are compared and the combination resulting with the highest isolator displacement control is indicated. The following conclusions are drawn based on the results obtained from the study.

1. Application of supplemental viscous, viscoelastic, and friction dampers in the base-isolated buildings generally decreases the isolator displacement.
2. Viscous dampers are most effective in mitigating large isolator displacement without adversely affecting other responses of the base-isolated building when damping ratio of damper (ξ_d) is between 10% and 25%.
3. Damping ratio (ξ_d) values of 15% to 25% and relative damper stiffness (k') values of 0.5 to 1.5 may be selected as optimum range of parameters where viscoelastic dampers are most effective in controlling isolator displacement without adverse effect on the other seismic responses.
4. Friction dampers are most effective in mitigating large isolator displacement without adversely affecting other responses of the base-isolated building for normalized limiting friction forces (μ_d) between 0.05 and 0.1.
5. Friction damper is found to result in lower isolator displacement as compared to the cases when viscous and viscoelastic dampers are used. However, the use of friction dampers also causes increase in top floor acceleration and storey shear.
6. The use of friction supplemental dampers in base-isolated building transfers more earthquake acceleration associated with high frequencies to the superstructure as compared to the viscous and viscoelastic dampers.
7. Viscous damper is found to provide improved control of isolator displacement without adversely affecting floor acceleration and storey shear as compared to that provided by the viscoelastic and friction dampers.
8. In combination with the supplemental dampers, the R-FBI experiences the lowest isolator displacement followed by the N-Z system under near-fault ground motions.
9. Base-isolated buildings subjected to near-fault ground motions benefit more from the use of supplemental dampers as compared to those subjected to the far-fault ground motions.

REFERENCES

1 Kelly JM (1986). “Aseismic Base Isolation: Review and Bibliography”. *Soil Dynamics and Earthquake Engineering*, **5**(3): 202-216.

2 Jangid RS and Datta TK (1995). “Seismic Behavior of Base-Isolated Building: A State-of-the-Art Review”. *Structures and Buildings*, **110**(2): 186-203.

3 Kelly JM and Hodder SB (1982). “Experimental Study of Lead and Elastomeric Dampers for Base Isolation Systems in Laminated Neoprene Bearings”. *Bulletin of the New Zealand National Society for Earthquake Engineering*, **15**(2): 53-67.

4 Shimoda I, Nakano S, Kitagawa Y and Miyazaki M (1988). “Experimental Study on Base-Isolated Building using Lead Rubber Bearing through Vibration Tests”. *Ninth World Conference on Earthquake Engineering*, Tokyo-Kyoto, Japan, 2 August - 9 August 1988, Volume 5, 711-716.

5 Mokha A, Constantinou MC, Reinhorn AM and Zayas VA (1991). “Experimental Study of Friction-Pendulum Isolation System”. *Journal of Structural Engineering*, **117**(4): 1201-1217.

6 Rao PB and Jangid RS (2001). “Experimental Study of Base-Isolated Structures”. *ISET Journal of Earthquake Technology*, **38**(1): 1-15.

7 Fenz DM and Constantinou MC (2006). “Behaviour of the Double Concave Friction Pendulum Bearing”. *Earthquake Engineering and Structural Dynamics*, **35**: 1403-1424.

8 Rabiei M and Khoshnoudian F (2011). “Response of Multistory Friction Pendulum Base-Isolated Buildings Including the Vertical Component of Earthquakes”. *Canadian Journal of Civil Engineering*, **38**: 1045-1059.

9 Nanda RP, Agarwal P and Shrikhande M (2012). “Suitable Friction Sliding Materials for Base Isolation of Masonry Buildings”. *Shock and Vibration*, **19**: 1327-1339.

10 Ponze FC, Cesare AD, Nigro D, Simonetti M and Leccese G (2014). “Shaking Table Tests of a Base Isolated Structure with Double Concave Friction Pendulums”. *Proceedings of the 2014 NZSEE Conference*, Auckland, New Zealand, 21 March - 23 March 2014, Paper No 43.

11 Hall JF, Heaton TH, Halling MW and Wald DJ (1995). “Near-Source Ground Motion and Its Effects on Flexible Buildings”. *Earthquake Spectra*, **11**(4): 569-605.

12 Jangid RS and Kelly JM (2001). “Base Isolation for Near-Fault Motions”. *Earthquake Engineering and Structural Dynamics*, **30**: 691-707.

13 Kelly JM (1999). “The Role of Damping in Seismic Isolation”. *Earthquake Engineering and Structural Dynamics*, **28**(1): 3-20.

14 Jangid RS (2005). “Optimum Friction Pendulum System for Near-Fault Motions”. *Engineering Structures*, **27**: 349-359.

15 Jangid RS (2007). “Optimum Lead-Rubber Isolation Bearings for Near-Fault Motions”. *Engineering Structures*, **29**: 2503-2513.

16 Makris N and Chang SP (1998). “Effect of Viscous, Viscoplastic and Friction Damping on the Response of Seismic Isolated Structures”. *ISET Journal of Earthquake Technology*, **35**(4): 113-141.

17 Zhang Y and Iwan WD (2002). “Protecting Base-Isolated Structures from Near-Field Ground Motion by Tuned

Interaction Damper". *Journal of Engineering Mechanics*, **128**: 287-295.

18 Lu LY and Lin GL (2009). "Improvement of Near-Fault Seismic Isolation using a Resettable Variable Stiffness Damper". *Engineering Structures*, **31**: 2097-2114.

19 Ozbulut OE, Bitaraf M and Hurlebaus S (2011). "Adaptive Control of Base-Isolated Structures against Near-Field Earthquakes using Variable Friction Dampers". *Engineering Structures*, **33**: 3143-3154.

20 Chang SP, Makris N, Whittaker AS and Thompson AC (2002). "Experimental and Analytical Studies on the Performance of Hybrid Isolation Systems". *Earthquake Engineering and Structural Dynamics*, **31**: 421-443.

21 Kim HS, Roschke PN, Lin PY and Loh CH (2006). "Neuro-Fuzzy Model of Hybrid Semi-Active Base Isolation System with FPS Bearings and an MR Damper". *Engineering Structures*, **28**: 947-958.

22 Lu LY and Lin GL (2008). "Predictive Control of Smart Isolation System for Precision Equipment Subjected to Near-Fault Earthquakes". *Engineering Structures*, **30**: 3045-3064.

23 Providakis CP (2008). "Effect of LRB Isolators and Supplemental Viscous Dampers on Seismic Isolated Buildings under Near-Fault Excitations". *Engineering Structures*, **30**: 1187-1198.

24 Lu LY, Lin CC and Lin GL (2013). "Experimental Evaluation of Supplemental Viscous Damping for Sliding Isolation System under Pulse-Like Base Excitations". *Journal of Sound and Vibration*, **332**: 1982-1999.

25 Oh SH, Song SH, Lee SH and Kim HJ (2013). "Experimental Study of Seismic Performance of Base-Isolated Frames with U-Shaped Hysteretic Energy-Dissipating Devices". *Engineering Structures*, **56**: 2014-2027.

26 Qin C, Liu W, and He W (2014). "Seismic Response Analysis of Isolated Nuclear Power Plants with Friction Damper Isolation". *2nd AASRI Conference on Power and Energy Systems*, Jeju Island, Korea, 27 December - 28 December 2013, Volume 7, Paper No 5, 26-31.

27 Wen, YK (1976). "Method for Random Vibrations of Hysteretic Systems". *Journal of Engineering Mechanics Division*, **102**: 249-263.

28 Zayas VA, Low SS and Mahin SA (1990). "A Simple Pendulum Technique for Achieving Seismic Isolation". *Earthquake Spectra*, **6**(2): 317-333.

29 Mostaghel N and Khodaverdian M (1987). "Dynamics of Resilient-Friction Base Isolator (R-FBI)". *Earthquake Engineering and Structural Dynamics*, **15**: 379-390.

30 Matsagar V, Jangid RS (2006). "Base-Isolated Building Connected to Adjacent Building using Viscous Dampers". *Bulletin of the New Zealand Society for Earthquake Engineering*, **39**(1): 59-80.